

GPO PRICE \$
CFSTI PRICE(S) \$
Hard copy (HC) \$2.00
Microfiche (MF) 150
ff 653 July 65

Solar Evolution With Varying G

D. Ezer and A.G.W. Cameron
Institute for Space Studies
Goddard Space Flight Center, NASA
New York, New York

Abstract

The model sequence calculations by the writers of early solar evolution have been extended to the case of a varying-G cosmology. In the varying-G sun there is less lithium depletion than in a constant-G sun, and the time required to burn out central hydrogen is decreased by less than the ratio of luminosities owing to the much greater total helium production in the varying-G sun. At the present time the varying-G model has four times the B^8 neutrino flux of the constant-G model, a prediction which can be subjected to an experimental check.

35729

FACILITY FORM 802

N66 35729
(ACCESSION NUMBER)

50
(PAGES)

TMX-56937
(NASA CR OR TMX OR AD NUMBER)

(THRU)
1

(CODE)
30

(CATEGORY)

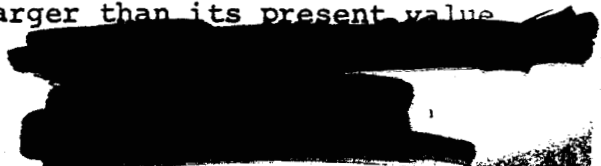
Introduction

There have been a number of attempts to incorporate Mach's Principle into general relativity. Perhaps the most promising of these is the attempt by R.H. Dicke and his colleagues to introduce a scalar field into general relativity in addition to the usual tensor field (Dicke 1964). Such a theory can be formulated in a variety of ways, but the most useful way appears to be a formulation in which particle masses remain unchanged with time, but in which the gravitational coupling coefficient G varies with time. The required rate of variation of G is so slow that the possibility has not yet been subjected to a definitive laboratory test. Consequently, it has been necessary to look for possible astronomical or geophysical tests of the idea of a varying G .

It appears that variations in G will have a great effect on stellar evolution. G enters into the equations of stellar structure through the equation of hydrostatic equilibrium:

$$\frac{dP}{dr} = - \frac{GM(r)\rho}{r^2} \quad (1)$$

where $M(r)$ is the mass inside radial distance r , ρ is the density and P is the pressure. When G is larger than its present value



the pressure gradient is correspondingly larger, and hence any structures calculated consistent with the equation of hydrostatic equilibrium are more compact. This means that the central temperatures of the stars would be larger, the opacity would be considerably reduced, and stellar luminosities are likely to be much greater than at the present time. In fact, Dicke has estimated that the luminosity of a star in radiative equilibrium might well vary as the seventh or eighth power of G .

Our present evolutionary study was motivated by two possible effects which a varying G would have upon the evolution of the sun. These effects have concerned the rate of destruction of lithium in the outer layers of the sun and the total evolutionary lifetime of the star of solar mass.

The essentials of the lithium problem are as follows. Lithium is observed to be depleted in the sun, relative to lithium in the meteorites, by at least 2 orders of magnitude (Shima and Honda 1963, Suess and Urey 1958). The question then arises as to whether the sun or the meteorites is normal. Some other stars are observed to have much more lithium than the sun; in fact their lithium abundances are quite comparable to those in meteorites. Cameron (1962) has suggested that the meteoritic abundance of lithium is normal, and that the sun and certain other stars have been depleted

in lithium to a great extent. On the other hand, Fowler, Greenstein, and Hoyle (1962) have suggested that the normal lithium abundance is extremely small in the matter out of which the solar system condensed, and that the amount present in the sun and in the meteorites was made by spallation and neutron capture processes taking place in the early history of the solar system. Thus it is of great interest to determine to what extent lithium would be depleted in the normal course of solar evolution by thermonuclear reactions.

We have recently shown (Ezer and Cameron 1965) that the early phases of evolution of the sun involve a fully convective object which contracts toward the main sequence. After some time, the central regions of the primordial sun change over to radiative equilibrium, and the lower boundary of the convection zone approaches the surface. There is still an outer convection zone in the sun, indicating that the sun has never been fully radiative. Lithium has certainly been destroyed toward the center of the sun, so that the question occurs as to whether it would ever be destroyed in that part of the outer layers which constitute the convective zone. Our recent study indicated that while the depletion of Li^6 was quite large during the contraction phase, the depletion of Li^7 was relatively minor, amounting to a factor of only 1.5.

There are many processes by which the depletion of lithium in the sun could have been more extensive than indicated in the above calculations. These processes include the effects of meridional circulation owing to a rapid early rotation of the sun, and a possible extensive mass loss of the outer layers of the sun. Meridional circulation would allow interchange of matter between the convective envelope and the inner parts of the sun which are in radiative equilibrium. Mass loss from the surface of the sun would carry away lithium into space; the remaining lithium would be diluted as the outer convection zone then extends into deeper layers. Neither of these questions have yet been quantitatively examined. However, Professor Dicke suggested to us that in the early contraction phases of the sun, if G is greater than at present, the interior luminosity of the sun would be also greatly increased, and this might cause the outer convection zone to extend to a greater depth at any given time during the contraction phase. His suggestion was therefore that a more extensive convection region in the early contraction phases would greatly increase the lithium depletion. This suggestion was one of the motivating factors in our decision to study solar evolution with varying G .

The question of the solar evolution lifetime is intimately connected with the abundance of helium in the sun and in the galaxy as a whole. In an expanding model universe of the type that Dicke suggests to be consistent with the variation of G , the present age of the universe is about 7×10^9 years, and hence the sun and solar system would have to be formed at the relatively early universe age of 2.5×10^9 years. This raises important questions concerning nucleosynthesis. If the universe goes through a high temperature-high density stage, then there is the possibility that the large abundance of helium in the sun and stars is of primordial origin (Peebles 1965). The alternate possibility that the helium has been manufactured in stellar interiors was recently considered by Truran, Hansen, and Cameron (1965). Their conclusion was that inadequate amounts of helium could be made in massive rapidly evolving stars, but that there was a possibility that sufficient amounts of helium might be made in stars of approximately solar mass. Most of the mass of the galaxy must be processed through such stars in order to manufacture the initial solar abundance of helium. The crucial question regarding the possibility of making helium in a more rapidly evolving universe, such as suggested by Dicke, thus involves the question of whether the lifetime of the sun would

be shortened to much less than 2.5×10^9 if the sun was formed rather early in the lifetime of the universe. Professor Dicke had suggested that such a shortened lifetime would occur as a result of the increase of G at earlier times. This has been a second motivating factor in the investigations reported in this paper.

The Variation of G

The general relativistic and cosmological equations which incorporate the scalar and tensor gravitational fields have been discussed by Brans and Dicke (1961). In such a cosmology G varies very rapidly in the early stages but much more slowly at later times. These variations of G must be determined by numerical integrations of equations 48 to 58 of the article of Brans and Dicke. During the earlier phases of the expansion an analytical solution may be used, which is given by equations 60 to 63 of the paper by Brans and Dicke. Professor Dicke has recommended to us the following sets of parameters which give a reasonable model of the expanding universe consistent with present experimental data:

$$\omega = 5$$

$$\text{present time} = 7.0 \times 10^9 \text{ years}$$

$$\text{decelleration parameter} - \ddot{a} a / \dot{a}^2 = 1.25$$

which yields at the present time

$$\dot{G}/G_0 = -2.01 \times 10^{-11} \text{ years}^{-1}$$

$$T_H = a/\dot{a} = \text{Hubble age} = 13.5 \times 10^9 \text{ years.}$$

Professor Dicke has provided us with numerical solutions to the cosmological equations for these parameters which have been obtained by Professor Peter Roll. Variation of G with time corresponding to this model is shown in Figure 1.

We have approximated the variation of G by the following expressions:

$$\frac{G}{G_0} = 1.010 \left(\frac{7.36}{T_9} \right)^{0.1083} \quad (2)$$

for the interval

$$0 < T_9 \leq 0.905;$$

$$\frac{G}{G_0} = 1.3943 - 0.1507 T_9 + 0.00664 T_9^2 + 0.00499 T_9^3 \quad (3)$$

for the interval

$$0.905 \leq T_9 \leq 2.50;$$

and

$$\frac{G}{G_0} = 1.25130 - 0.05116 T_9 + 0.00218 T_9^2 \quad (4)$$

for the interval

$$T_9 \geq 2.50$$

Results and Discussion

Evolutionary sequences of solar models were constructed in the same manner as described in our previous paper (Ezer and Cameron 1965). The only modification used was the treatment of G as a variable rather than as a constant in the equations.

There is a conceptual error associated with this treatment which, however, does not make a significant error in the final results.

The gravitational potential energy of the sun is proportional to G . According to the virial theorem, the binding energy of the sun is half the gravitational potential energy. Hence, as G decreases with time, the binding energy of the sun should also decrease with time. The only source of energy to supply this decrease in the binding energy is the scalar gravitational field itself. Consequently, a complete theory of stellar structure in the presence of varying G would include an energy input to the sun due to the variation of the scalar field. Such an energy input term was not included because the nuclear energy released in the solar interior during the sun's lifetime is orders of magnitude greater than the scalar field variation energy input. Consequently, the neglect of this extra term can have very little effect on

the final results.

The evolution of the sun was started at the universe age $T_0 = 2.5 \times 10^9$ years. The evolution was started at the threshold of stability, at which the gravitational potential energy of the sun is just sufficient to supply the internal thermal energy, the dissociation energy of hydrogen molecules, and the necessary amount of ionization energy of hydrogen and helium in the interior. The solar models were followed through the contraction stage onto the main sequence, and then through the period of hydrogen burning until hydrogen was just exhausted at the center.

The characteristics of representative models are given in Table 1. In this table the first column gives the solar evolution time in years measured from the threshold of stability. The second and third columns give the radius and luminosity of the model in present solar units. The fourth column gives the logarithm of the effective temperature of the model, and the fifth column gives the photospheric density in grams per cubic centimeter. The remaining columns give, respectively, the central density in grams per cubic centimeter, the central temperature in $^{\circ}\text{K}$, the fractional mass of hydrogen at the center of the sun, and the relative contribution of the gravitational energy release to the total energy flowing out of the sun.

The luminosity is plotted as a function of the effective temperature in Figure 2. In this figure the dashed line represents the track which has previously been found for the sun without any variation of G ; this track has here been extended to the point where the central hydrogen has been depleted in the sun at a time of 10^{10} years, and through the subsequent formation of a hydrogen-burning shell source and evolution up to an age of 1.4×10^{10} years. The solid line shows the track followed by the sun with variation of G . It may be seen that this line lies at slightly higher effective temperatures than in the constant G case. Furthermore, the solid line turns toward the upper left at a higher luminosity than for constant G , and it intersects the main sequence position also at a higher luminosity. After reaching the main sequence, the line curves down toward the lower right, and at an age of 4.5×10^9 years it has about the same effective temperature as the sun, but the luminosity is about 20% too high. Hydrogen is exhausted at the center at an age of 9.8×10^9 years; the track turns up slightly before this point is reached.

As in the case with constant G , the nearly vertical contraction path of the early sun represents models which are fully convective. The tracks turn up toward the lower left after a central radiative core has formed in the models and as this

radiative core grows to take in most of the mass of the star. After the sun has become mostly radiative, a small central convective core forms, grows until a maximum size is reached, and then gradually disappears. The characteristics at the boundaries of the radiative and convective regions are shown in Table 2. In this table the first column again gives the solar evolution time in years. The other columns give the characteristics of the boundary between a radiative and a convective region. The first sequence of values refers to the top of the central radiative core; the later values refer to the top of the central convective core after the bulk of the star has become radiative. The second and subsequent columns give the fractional mass of the core at the boundary, the fractional radius of the boundary, the boundary temperature in $^{\circ}\text{K}$, and the boundary density in grams per cubic centimeter.

This table may be compared with Table 6a of Ezer and Cameron (1965). Such a comparison indicates that, relative to the models with constant G , the models with varying G start to develop a radiative core at the center sooner. At a given luminosity the models have a larger radius and a lower central density. The resulting low opacities cause a development of a radiative core at the center of the sun at considerably lower temperatures than for the constant G cases. The temperature at the bottom of the

convective zone decreases as the convective zone recedes toward the surface; the temperature thus never reaches high values.

This behavior results in less lithium burning in the varying G models than in the constant G models. We have determined by an approximate numerical calculation that Li^7 is depleted by only 10% in the outer convective zone of the sun with varying G. Thus our first significant conclusion is that a variety of effects associated with the complicated behavior of stellar opacities conspire to invalidate the simple prediction which Dicke made concerning lithium burning.

The decrease of the luminosity and of the effective temperature during the main sequence hydrogen burning phase of the sun with varying G is an effect which has already been found by Pochoda and Schwarzschild (1964). It may be noted that the models have too large a luminosity by some 20% at the sun's age of 4.5×10^9 years. We estimate that the luminosity would have come out correctly if the helium content by mass of the initial sun had been reduced from the assumed value of 24% to about 22%. This alternate choice of helium content would be quite consistent with the uncertainties in the hydrogen-to-helium ratio in the sun.

It is at first sight surprising to find that the models with constant G and with varying G both take very nearly 10^{10} years

to burn out their central hydrogen, despite the fact that the models with varying G have a much higher luminosity throughout most of the solar lifetime. This can occur only if much more hydrogen has been consumed in the interior of the sun at the time of central hydrogen burnout for the varying G case than for the constant G case.

We have investigated this point in several ways. Figure 3 shows the ratios of the net rates of destruction of hydrogen by the two branches of the proton-proton chain. $r_{3,4}$ is the rate of the $\text{He}^3(\alpha, \gamma)\text{Li}^7$ reaction. The branch of the proton-proton chain containing this reaction makes one He^4 nucleus per one basic proton-proton reaction. The rate $r_{3,3}$ is the rate of the $\text{He}^3(\text{He}^3, 2p)\text{He}^4$ reaction. In this branch of the proton-proton chain the formation of one He^4 nucleus requires two basic proton-proton reactions. The ratio $r_{3,4}/(r_{3,4} + 2r_{3,3})$ increases with temperature and He_4 content. It may be seen that when this ratio is high, a greater fraction of the luminosity of the sun will be supplied by the material at the very center, and hence the material at the center will burn out relatively sooner. Figure 3 shows this ratio for the varying G and constant G cases very early in solar evolution on the main sequence. It may be seen that in the constant G case this ratio is rather small but has a fairly sharp

peak toward the center. In the varying G case, the ratio is higher and has a much broader flat peak at the center associated with larger central convection zone in the sun.

Figure 4 shows the fraction by mass of helium in the present sun, corresponding to the age 4.5×10^9 years, for both the varying G and the constant G cases. It may be seen that much more helium has been formed for the varying G case than for the constant G case, as was expected. It may also be seen that the excess helium extends very significantly to larger mass fractions. Figure 5 shows a similar plot for the two cases with the central hydrogen just depleted. Here it may be seen that in the constant G case the central hydrogen is depleted just at the very center of the star and the hydrogen content then rapidly increases away from the center. In the varying G cases, however, hydrogen has burned out nearly uniformly over a fairly wide region, and hydrogen then increases away from this flat plateau. The amount of helium formed in the sun with varying G is much greater than that with constant G, and this indicates why the two model sequences can take nearly the same time to burn out the central hydrogen.

We have found some significant differences in the spectrum of neutrinos emitted from the present sun in the constant G and varying G cases. Table 3 shows the neutrino fluxes at one

astronomical unit for the solar models with constant G which were reported in our previous paper (Ezer and Cameron 1965). The first four columns give the evolutionary age of the sun in years, the radius in solar units, the luminosity in solar units, and the central fractional mass of hydrogen. The subsequent columns give the neutrino flux from the reactions $H^1(p, \beta^+ \nu) D^2$, $Be^7(e^-, \nu) Li^7$, $B^8(\beta^+ \nu) Be^{8*}$, $N^{13}(\beta^+ \nu) C^{13}$, and $O^{15}(\beta^+ \nu) N^{15}$. The last column gives the total neutrino flux. Table 4 gives a similar set of numbers for the solar models with varying G . In order to compare Tables 3 and 4 at 4.5×10^9 years, it would appear appropriate to decrease the neutrino fluxes in Table 4 by about 20%.

On this basis the present sun with varying G emits approximately four times as many neutrinos from the decay of B^8 as does the present sun with constant G . This difference has particular significance in view of the fact that the large solar neutrino detection experiment of R. Davis (1964), consisting of a large underground tank containing a chlorine compound in which solar neutrinos produce radioactive A^{37} , is most sensitive to the B^8 neutrinos from the sun. His experiment, which is now in preparation, is expected to detect the solar neutrino flux, and therefore there is a real possibility that it will constitute a test of the variation or nonvariation of G if solar models can be sufficiently refined

so that there is agreement about the expected neutrino flux in either of the cases. It may be noted that the best prediction of the B^8 neutrinos for the present sun with constant G due to Sears (1964) gives a value which is intermediate between the two numbers given in Tables 3 and 4.

The failure of the solar model with varying G to burn out its central hydrogen significantly faster than the solar model with constant G raised questions in our mind concerning the possible role of stars of about solar mass in the earlier history of the universe in the cosmology in which G varies. Consequently, calculations of the evolutionary tracks were repeated, starting the sun at the threshold of stability at universe ages $T_0 = 0.5 \times 10^9$ years and $T_0 = 0.1 \times 10^9$ years. The results are displayed in Tables 5 through 8. Tables 5 and 6 are equivalent to Tables 1 and 2, respectively, for the models starting with $T_0 = 0.5 \times 10^9$ years. Similarly, Tables 7 and 8 are equivalent to Tables 1 and 2 for the models starting with $T_0 = 0.1 \times 10^9$ years. In these models G is initially larger than in the previously calculated models, and consequently the central temperatures in the initial sun are higher. For the case $T_0 = 0.1 \times 10^9$ years, the carbon-nitrogen-oxygen cycles of nuclear reactions make significant contributions to the energy generation in the center.

The evolutionary tracks and the luminosity-effective temperature diagram are shown in Figure 6. It may be seen that the models starting at smaller universe ages go to significantly higher luminosities and effective temperatures than would be the case for the present sun with varying G . The tracks then exhibit much more extensive movement toward lower luminosities and effective temperatures. The maximum mass fraction of the central convective core extends to 17% and 28% of the mass for $T_0 = 0.5 \times 10^9$ years and 0.1×10^9 years, as compared to 13% of the mass for the case $T_0 = 2.5 \times 10^9$ years. The times required for depletion of the central hydrogen in the cases $T_0 = 0.5 \times 10^9$ years and 0.1×10^9 years are 3.5×10^9 years and 2.4×10^9 years. It may be seen that the first of these cases has a marked reduction in this burn-out time as compared to $T_0 = 2.5 \times 10^9$ years. However, there is not much additional reduction in lifetime for the case $T_0 = 0.1 \times 10^9$ years, presumably owing to the much greater extent of the central convective core in these models. The more extensive central hydrogen burning which takes place in these other model sequences is indicated in Figure 7. It may be seen that the earlier the sun starts to evolve in the age of the universe, the greater is the burn-out of hydrogen in the interior at the time hydrogen becomes exhausted at the center.

These results are particularly significant in connection with a question of helium formation in the galaxy. For the case of stellar evolution with constant G , Truran, Hansen, and Cameron (1965) have shown that massive stars can contribute very little helium to the interstellar medium, but there is a chance that the large amount of helium in the sun could have been made as a result of stellar evolution in stars of approximately solar mass. However, the associated universe ages must be rather long and the fraction of initial galactic gas that must be processed is large. The present results indicate that such stellar helium production is very difficult in this varying G cosmology. Thus the large amount of helium in the initial sun may have to be attributed to primordial processes (Peebles 1965).

References

- Brans, C., and Dicke, R.H. 1961. Phys. Rev. 124, 925.
- Cameron, A.G.W. 1962. Icarus, 1, 13.
- Davis, R., Jr. 1964. Phys. Rev. Letters, 12, 302.
- Dicke, R.H. 1964. The theoretical significance of experimental relativity. (Gordon and Breach, New York).
- Ezer, D., and Cameron, A.G.W. 1965. Can. J. Phys. 43, 1497.
- Fowler, W.A., Greenstein, J.L., and Hoyle, F. 1962. Geophys. J. 6, 148.
- Peebles, P.J.E. 1965. preprint.
- Pochoda, P., and Schwarzschild, M. 1964. Astrophys. J. 139, 587.
- Sears, R.L. 1964. Astrophys. J. 140, 477.
- Shima, M. and Honda, M. 1963. J. Geophys. Res. 68, 2849.
- Suess, H.E., and Urey, H.C. 1958. Handb. der Physik, 51, 296.
- Truran, J.W., Hansen, C.J., and Cameron, A.G.W. 1965. Can. J. Phys. 43, 1616.

TABLE 1

Evolutionary sequence of solar models with varying G and beginning of evolution at a universe age $T_0 = 2.5 \times 10^9$ years.

time (yrs)	R/R_\odot	L/L_\odot	$\log T_e$	$\rho_{ph} \left(\frac{gm}{cm^3} \right)$	$\rho_c \left(\frac{gm}{cm^3} \right)$	T_c	X_1	L_q/L
3.17	70.6	842.	3.571	7.11×10^{-9}	4.44×10^{-5}	1.41×10^5	0.739	1.000
9.51	68.9	818.	3.572	7.12	4.75	1.45	"	"
1.58×10	67.3	790.	3.574	7.20	5.06	1.48	"	"
2.22	65.8	763.	3.575	7.28	5.36	1.51	"	"
3.49	63.1	709.	3.576	7.53	5.97	1.57	"	"
6.02	58.9	639.	3.580	7.79	7.14	1.67	"	"
1.11×10^2	53.0	543.	3.585	8.22	9.44	1.85	"	"
2.12	45.8	435.	3.593	8.84	1.40×10^{-4}	2.11	"	"
4.15	38.0	323.	3.601	9.89	2.29	2.51	"	"
8.21	30.7	231.	3.611	1.13×10^{-8}	4.11	3.06	"	"
1.63×10^3	24.3	159.	3.621	1.33	7.87	3.80	"	"
3.26	19.0	108.	3.633	1.58	1.58×10^{-3}	4.81	"	"
6.50	14.7	71.4	3.644	1.95	3.27	6.13	"	"
1.30×10^4	11.3	46.5	3.653	2.45	6.84	7.85	"	"
1.95	9.65	35.6	3.659	2.82	1.09×10^{-2}	9.16	"	"
3.25	7.96	25.3	3.664	3.38	1.89	1.10×10^6	"	"

TABLE 1 (continued)

Time (yrs)	R/R_{\odot}	L/L_{\odot}	$\log T_e$	$\rho_{ph} \left(\frac{gm}{cm^3} \right)$	$\rho_c \left(\frac{gm}{cm^3} \right)$	T_c	X_1	L_g/L
1.92	1.13	1.81	3.800	7.46	7.97	1.53	.739	.100
1.26	1.07	1.59	3.794	8.21	7.86	1.54	.738	.026
1.92	1.06	1.62	3.803	7.72	8.65	1.57	.738	.072
3.30	1.06	1.68	3.807	7.23	9.29	1.60	.737	.090
3.96	1.05	1.68	3.808	7.13	9.51	1.61	.736	.023
5.29	1.05	1.67	3.808	7.15	9.58	1.61	.736	.003
7.95	1.05	1.67	3.808	7.15	9.65	1.61	.731	.001
1.33×10^8	1.05	1.66	3.808	7.19	9.75	1.62	.724	.001
2.39	1.05	1.65	3.806	7.32	9.93	1.62	.710	.001
4.52	1.05	1.62	3.804	7.60	1.03×10^2	1.63	.682	.001
8.77	1.05	1.55	3.800	8.18	1.10	1.64	.629	.001
1.30×10^9	1.05	1.49	3.795	8.76	1.18	1.65	.576	.001
1.73	1.05	1.43	3.791	9.34	1.27	1.66	.523	.001
2.15	1.05	1.38	3.787	9.91	1.38	1.68	.471	.001
2.57	1.05	1.34	3.784	1.04×10^{-7}	1.51	1.70	.419	.001
3.00	1.05	1.30	3.780	1.09	1.65	1.72	.367	.000
3.43	1.06	1.27	3.777	1.14	1.82	1.74	.317	.000

TABLE 1 (continued)

Time (yrs)	R/R _⊙	L/L _⊙	log T _e	$\rho_{ph} \left(\frac{gm}{cm^3} \right)$	$\rho_c \left(\frac{gm}{cm^3} \right)$	T _c	X ₁	L _q /L
1.86	1.06	1.24	3.774	1.19	2.01	1.77	.267	.000
1.28	1.06	1.21	3.772	1.23	2.24	1.80	.219	.000
1.50	1.06	1.20	3.770	1.25	2.39	1.82	.191	.000
1.94	1.07	1.19	3.768	1.29	2.68	1.86	.141	.000
1.82	1.08	1.16	3.763	1.36	3.31	1.94	.062	.000
1.38	1.10	1.18	3.761	1.34	4.72	1.83	.016	.001
1.50	1.14	1.22	3.758	1.33	6.32	1.82	.003	.000
1.76	1.23	1.38	3.754	1.26	8.77	1.87	.000	-.001

TABLE 2

The physical characteristics at the boundaries of the radiative and convective regions for evolutionary models with varying G and beginning of evolution at a universe age $T_0 = 2.5 \times 10^8$ years.

Time (yrs)	M_{core}/M		r_{core}/R		$T_b (^{\circ}\text{K})$		$\rho_b (\text{gm cm}^{-3})$	
	conv.	rad.	conv.	rad.	conv.	rad.	conv.	rad.
9.67×10^5		.01		.12		3.44×10^6		0.62
1.80×10^6		.17		.32		3.43		0.82
2.63		.33		.42		3.35		0.92
4.29		.49		.48		3.31		1.03
5.95		.63		.54		3.17		0.96
9.28		.85		.64		2.60		0.52
1.09×10^7		.91		.66		2.43		0.33
1.43		.99		.75		1.55		0.04
1.59	.004		.03		1.31×10^7		7.69×10	
1.67	.06		.08		1.25		6.73	
1.76	.10		.10		1.22		6.11	
1.92	.13		.12		1.20		5.52	
2.26	.13		.13		1.23		5.60	
2.92	.09		.11		1.32		6.63	
3.30	.06		.10		1.39		7.53	

TABLE 2 (continued)

Time (yrs)	M _{core} /M		r _{core} /R		T _b (°K)		ρ _b (gm/cm ³)	
	conv.	rad.	conv.	rad.	conv.	rad.	conv.	rad.
3.96 x 10 ⁷	.05		.09		1.42		7.92	
5.29	.04		.08		1.44		8.09	
7.95	.04		.08		1.44		8.20	
1.33 x 10 ⁸	.04		.08		1.45		8.30	
2.39	.04		.08		1.45		8.44	
4.52	.04		.08		1.46		8.73	
8.77	.04		.08		1.47		9.34	
1.30 x 10 ⁹	.03		.07		1.48		1.01 x 10 ²	
1.73	.02		.05		1.50		1.10	
2.15	.02		.06		1.52		1.20	
2.57	.02		.06		1.54		1.31	
3.00	.02		.05		1.57		1.44	
3.43	.015		.05		1.59		1.60	
3.86	.010		.04		1.63		1.78	
4.28	.010		.04		1.66		2.00	
4.50	.008		.035		1.69		2.14	
4.94	.007		.03		1.73		2.42	
5.82	.003		.023		1.83		3.03	

TABLE 3

Neutrino fluxes at 1 astronomical unit $\text{cm}^{-2} \text{sec}^{-1}$
for evolutionary solar models with constant G.

Time (yrs.)	R/R _⊙	L/L _⊙	X ₁	ν_{pp}	ν_{Be^7}	ν_{Be^8}	$\nu_{\text{N}^{13}}$	$\nu_{\text{O}^{15}}$	ν_{total}
91 x 10 ⁹	0.903	0.822	0.616	5.30 x 10 ¹⁰	2.49 x 10 ⁹	1.35 x 10 ⁶	2.23 x 10 ⁸	1.06 x 10 ⁸	5.58 x 10 ¹⁰
34	.923	.876	.548	5.54	3.63	2.74	2.80	1.81	5.95
18	.946	.932	.473	5.75	5.22	5.45	4.02	3.15	6.34
50	.966	.980	.409	5.91	6.94	9.48	5.97	5.13	6.72
50	1.034	1.155	.279	6.13	1.32 x 10 ¹⁰	3.72 x 10 ⁷	2.20 x 10 ⁹	2.15 x 10 ⁹	7.89
77	1.053	1.202	.226	6.09	1.46	4.77	3.41	3.36	8.23
20	1.064	1.227	.195	6.02	1.52	5.27	4.37	4.31	8.41
27	1.067	1.235	.185	5.98	1.53	5.40	4.75	4.69	8.46
34	1.070	1.240	.173	5.94	1.54	5.53	5.14	5.08	8.51
50	1.074	1.251	.162	5.92	1.55	5.66	5.54	5.49	8.58
51	1.080	1.262	.140	5.84	1.56	5.79	6.33	6.28	8.67
14	1.093	1.281	.097	5.64	1.54	5.87	8.14	8.09	8.81
11	1.122	1.319	.026	5.32	1.51	5.74	1.14 x 10 ¹⁰	1.13 x 10 ¹⁰	9.10
11 x 10 ¹⁰	1.170	1.451	.000	5.25	1.66	6.99	1.57	1.56	10.04

TABLE 4

Neutrino fluxes at 1 astronomical unit $\text{cm}^{-2} \text{sec}^{-1}$ for solar models with varying G and beginning of evolution at a universe age $T_0 = 2.5 \times 10^9$ years.

me rs.)	R/R_\odot	L/L_\odot	X_1	ν_{pp}	ν_{Be^7}	ν_{B^8}	$\nu_{\text{N}^{13}}$	$\nu_{0^{15}}$	ν_{total}
30×10^9	1.054	1.489	0.576	8.69×10^{10}	1.08×10^{10}	3.65×10^7	1.68×10^9	1.58×10^9	10.10×10^{10}
73	1.054	1.434	.523	8.20	1.16	4.06	1.80	1.73	9.72
15	1.054	1.384	.471	7.75	1.26	4.49	2.00	1.95	9.41
58	1.054	1.339	.419	7.33	1.32	4.84	2.26	2.22	9.10
00	1.054	1.306	.367	6.95	1.38	5.14	2.64	2.60	8.86
43	1.055	1.267	.317	6.60	1.41	5.24	3.12	3.09	8.64
86	1.058	1.238	.267	6.28	1.42	5.18	3.78	3.75	8.46
28	1.061	1.215	.219	5.97	1.42	4.90	4.63	4.61	8.32
50	1.063	1.205	.191	5.82	1.40	4.66	5.20	5.18	8.26
94	1.068	1.187	.141	5.50	1.35	4.10	6.45	6.43	8.14
82	1.080	1.159	.062	4.92	1.25	3.17	9.09	9.08	7.99
38	1.199	1.185	.016	5.06	1.38	3.50	8.64	8.63	8.17
50	1.135	1.226	.003	4.86	1.48	4.21	1.06×10^{10}	1.06×10^{10}	8.46
76	1.230	1.221	.000	4.19	1.49	5.40	1.98	1.98	9.62

TABLE 5

Evolutionary sequence of solar models with varying G and beginning of evolution at a universe age $T_0 = 0.5 \times 10^9$ years.

Time (yrs.)	R/R_\odot	L/L_\odot	$\log T_e$	$\rho_{ph} \left(\frac{gm}{cm^3} \right)$	$\rho_c \left(\frac{gm}{cm^3} \right)$	T_c	X_1	L_g/L
3.17	7.51×10	1.03×10^3	3.579	6.20×10^{-9}	3.38×10^{-5}	1.54×10^5	0.739	1.000
9.51	7.32	9.95×10^2	3.581	6.29	3.63	1.58	"	"
2.22×10	6.96	9.18	3.583	6.51	4.13	1.66	"	"
4.75	6.43	8.11	3.587	6.84	5.11	1.79	"	"
9.83	5.71	6.76	3.593	7.34	7.03	2.00	"	"
2.00×10^2	4.86	5.30	3.601	8.04	1.09×10^{-4}	2.32	"	"
4.03	3.99	3.90	3.611	9.10	1.86	2.78	"	"
8.08	3.19	2.76	3.622	1.06×10^{-8}	3.46	3.43	"	"
1.62×10^3	2.51	1.90	3.634	1.24	6.86	4.32	"	"
3.24	1.94	1.28	3.646	1.52	1.42×10^{-3}	5.50	"	"
6.49	1.50	8.42×10	3.657	1.90	2.98	7.06	"	"
1.30×10^4	1.15	5.47	3.667	2.38	6.33	9.07	"	"
2.60	8.88×10^0	3.54	3.677	3.02	1.35×10^{-2}	1.17×10^6	"	"
5.19	6.85	2.23	3.685	3.83	2.88	1.51	"	"
1.04×10^5	5.30	1.47	3.693	4.88	6.13	1.94	"	"
2.08	4.11	9.33×10^0	3.699	6.25	1.70×10^{-1}	2.49	"	"

TABLE 5 (continued)

Time (yrs.)	R/R _☉	L/L _☉	log T _e	$\rho_{ph}(\frac{gm}{cm^3})$	$\rho_c(\frac{gm}{cm^3})$	T _c	X ₁	L/L _g
12	3.51	7.13	3.704	7.24	2.07	2.91	"	"
19	2.92	4.92	3.704	8.93	3.62	3.44	"	"
35	2.39	3.33	3.705	1.11×10^{-7}	7.17	4.06	"	"
35×10^6	2.11	2.65	3.707	1.26	1.17×10^0	4.53	"	"
18	1.83	2.07	3.711	1.44	2.38	5.25	"	"
84	1.63	1.99	3.732	1.37	7.42	6.83	"	"
101	1.63	2.05	3.736	1.33	8.21	7.00	"	"
134	1.63	2.19	3.744	1.24	9.95	7.36	"	0.999
101	1.67	2.63	3.758	1.04	1.50×10^1	8.28	"	.998
34	1.87	4.87	3.800	4.44×10^{-8}	3.98	1.16×10^7	"	.983
00	1.79	6.17	3.834	2.40	5.97	1.38	"	.939
33	1.67	6.58	3.856	1.67	6.66	1.53	"	.834
00	1.47	5.82	3.871	1.46	6.48	1.66	"	.375
70	1.36	4.91	3.862	1.68	6.26	1.70	"	.120
45	1.31	4.43	3.867	1.88	6.22	1.71	"	.065
103×10^7	1.22	4.27	3.873	1.82	6.50	1.73	.738	.126

TABLE 5 (continued)

Time (yrs.)	R/R_{\odot}	L/L_{\odot}	$\log T_e$	$\rho_{ph} \left(\frac{gm}{cm^3} \right)$	$\rho_c \left(\frac{gm}{cm^3} \right)$	T_c	X_1	L_g/L
1.12	1.25	4.59	3.880	1.50	7.16	1.78	.738	.215
1.31	1.19	4.88	3.897	1.10	8.44	1.85	.738	.171
1.58	1.16	4.81	3.903	1.01	8.82	1.90	.737	.058
1.81	1.14	4.71	3.903	1.02	8.84	1.91	.736	.014
2.13	1.14	4.67	3.903	1.03	8.85	1.91	.736	.005
2.64	1.14	4.64	3.902	1.05	8.87	1.92	.734	.003
3.49	1.14	4.60	3.901	1.07	8.90	1.92	.732	.002
4.92	1.14	4.54	3.899	1.11	8.95	1.92	.728	.002
7.44	1.14	4.44	3.896	1.18	9.02	1.91	.721	.001
1.22×10^8	1.15	4.28	3.890	1.33	9.15	1.91	.708	.001
2.12	1.17	4.01	3.880	1.61	9.40	1.90	.685	.001
3.93	1.21	3.62	3.863	2.20	9.89	1.89	.642	.001
6.59	1.24	3.27	3.845	2.99	1.06×10^2	1.89	.502	.001
9.31	1.27	2.99	3.831	3.79	1.14	1.89	.522	.001
1.21×10^9	1.28	2.75	3.820	4.55	1.24	1.90	.462	.000
1.49	1.29	2.57	3.811	5.27	1.34	1.92	.402	.000

TABLE 5 (continued)

Time (yrs.)	R/R_{\odot}	L/L_{\odot}	$\log T_e$	$\rho_{ph} \left(\frac{gm}{cm^3} \right)$	$\rho_c \left(\frac{gm}{cm^3} \right)$	T_c	x_1	L_g/L
1.78	1.30	2.46	3.805	5.80	1.45	1.94	.342	.000
1.92	1.31	2.43	3.802	6.08	1.51	1.96	.312	.000
2.19	1.32	2.37	3.797	6.56	1.63	2.00	.253	.000
2.33	1.33	2.33	3.794	6.85	1.70	2.02	.223	.000
2.60	1.34	2.25	3.788	7.43	1.86	2.06	.165	.000
2.73	1.34	2.20	3.785	7.83	1.96	2.09	.136	-.001
3.00	1.35	2.13	3.781	8.32	2.23	2.16	.077	.000
3.28	1.35	2.10	3.778	8.66	2.65	2.26	.031	.000
3.43	1.37	2.19	3.781	8.13	3.35	2.40	.008	.003
3.47	1.39	2.35	3.785	7.38	4.61	2.44	.002	.012
3.48	1.42	2.53	3.789	6.76	6.48	2.46	.000	.057

TABLE 6

The physical characteristics at the boundaries of the radiative and convective regions for evolutionary models with varying G and beginning of evolution at a universe age $T_0 = 0.5 \times 10^9$ years.

Time (yrs.)	M_{core}/M		r_{core}/R		$T_b (^{\circ}\text{K})$		$\rho_b \text{ (gm/cm}^3\text{)}$	
	conv.	rad.	conv.	rad.	conv.	rad.	conv.	rad.
5.19×10^5		.05		.21		3.14×10^6		3.05×10^{-1}
9.35		.26		.38		3.07		3.85
1.35×10^6		.38		.44		3.09		4.57
2.18		.58		.53		2.95		4.73
3.84		.84		.64		2.49		2.55
4.01		.85		.64		2.48		2.46
4.34		.88		.65		2.32		1.94
5.01		.94		.69		1.97		2.52×10^{-2}
6.34		.999		.88		5.17×10^5		6.46×10^{-4}
7.00								
7.33	.02		.05		1.41×10^7		5.91×10^1	
8.00	.13		.10		1.31		4.53	
8.70	.17		.12		1.28		4.08	
9.45	.17		.13		1.29		4.09	
1.03×10^7	.15		.12		1.32		4.37	

TABLE 6 (continued)

Time (yrs.)	M _{core} /M		r _{core} /R		T _b (°K)		ρ _b (gm/cm ³)	
	conv.	rad.	conv.	rad.	conv.	rad.	conv.	rad.
1.12	.13		.12		1.41		5.06	
1.31	.07		.09		1.59		6.73	
1.58	.09		.10		1.59		6.77	
1.81	.10		.11		1.57		6.61	
2.13	.11		.11		1.56		6.51	
2.64	.11		.11		1.55		6.43	
3.49	.12		.12		1.54		6.38	
4.92	.12 q		.12		1.54		6.42	
7.44	.12		.12		1.53		6.46	
1.22 x 10 ⁸	.12		.11		1.53		6.54	
2.12	.12		.11		1.52		6.74	
3.93	.11		.10		1.51		7.09	
6.59	.10		.09		1.52		7.65	
9.31	.09		.09		1.52		8.27	

TABLE 6 (continued)

Time (yrs.)	M _{core} /M		r _{core} /R		T _b (°K)		ρ _b (gm/cm ³)	
	conv.	rad.	conv.	rad.	conv.	rad.	conv.	rad.
1.21 × 10 ⁹	.08		.08		1.53		8.94	
1.49	.08		.08		1.54		9.64	
1.78	.07		.07		1.55		1.03 × 10 ²	
1.92	.07		.07		1.56		1.06	
2.19	.07		.07		1.56		1.13	
2.33	.07		.07		1.56		1.16	
2.60	.07		.07		1.57		1.24	
2.73	.07		.06		1.58		1.28	
3.00	.06		.06		1.60		1.42	
3.28	.06		.06		1.67		1.67	
3.43	.05		.05		1.83		2.22	
3.47	.02		.03		2.11		3.69	
3.48	.005		.02		2.26		5.70	

TABLE 7

Evolutionary sequence of solar models with varying G and beginning of evolution at a universe age $T_0 = 0.1 \times 10^9$ years.

Time (yrs.)	R/R_\odot	L/L_\odot	$\log T_e$	$\rho_{ph} \left(\frac{gm}{cm^3} \right)$	$\rho_c \left(\frac{gm}{cm^3} \right)$	T_c	X_1	L_g/L
1.17	1.26×10^2	2.26×10^3	3.552	4.64×10^{-9}	8.59×10^{-6}	9.28×10^4	0.739	1.000
1.51	1.14	1.94	3.557	4.92	1.11×10^{-5}	1.03×10^5	"	"
1.22 x 10	9.97×10	1.58	3.564	5.31	1.59	1.17	"	"
1.75	8.41	1.22	3.573	5.84	2.50	1.39	"	"
1.83	6.86	8.97×10^2	3.583	6.57	4.29	1.68	"	"
1.00×10^2	5.47	6.34	3.595	7.52	7.86	2.07	"	"
1.03	4.30	4.36	3.607	8.71	1.52×10^{-4}	2.60	"	"
3.08	3.33	2.96	3.620	1.02×10^{-8}	3.07	3.30	"	"
1.62×10^3	2.57	1.97	3.632	1.23	6.38	4.21	"	"
3.24	1.97	1.31	3.645	1.50	1.36×10^{-3}	5.42	"	"
5.49	1.51	8.54×10	3.657	1.89	2.91	7.00	"	"
1.30×10^4	1.16	5.52	3.667	2.37	6.24	9.04	"	"
2.60	8.90×10^0	3.57	3.677	3.00	1.34×10^{-2}	1.17×10^6	"	"
5.19	6.85	2.30	3.686	3.81	2.88	1.51	"	"
1.04×10^5	5.30	1.47	3.693	4.88	6.13	1.94	"	"
2.08	4.11	9.31×10^0	3.699	6.26	1.29×10^{-1}	2.49	"	"
				8.07	2.71	3.17	"	"

TABLE 7 (continued)

Time (yrs)	R/R_{\odot}	L/L_{\odot}	$\log T_e$	$\rho_{ph} \left(\frac{gm}{cm^3} \right)$	$\rho_c \left(\frac{gm}{cm^3} \right)$	T_c	X_1	L_q/L
8.31	2.52	3.70	3.705	1.05×10^{-7}	6.00	3.89	"	"
1.66×10^6	2.01	2.44	3.709	1.32	1.50×10^0	4.75	"	"
3.32	1.67	1.97	3.726	1.42	5.12	6.23	"	"
4.99	1.67	2.66	3.759	1.03	1.60×10^1	8.51	"	.997
5.82	1.83	3.95	3.782	6.37×10^{-8}	2.78	1.02×10^7	"	.992
6.65	1.89	5.57	3.812	3.49	4.88	1.25	"	.972
7.0625	1.79	6.30	3.837	2.27	6.15	1.40	"	.931
7.0633	1.57	2.49×10	4.015	7.28×10^{-10}	9.30	1.96	"	-1.913
7.0642	1.57	2.53	4.016	7.18	9.10	1.97	"	-1.948
7.0658	1.57	2.55	4.017	7.14	8.79	1.99	"	-2.078
7.0691	1.57	2.52	4.016	7.20	8.32	2.00	"	-2.188
7.0758	1.56	2.43	4.014	7.42	7.68	2.01	"	-2.082
7.089	1.54	2.26	4.009	7.88	6.92	2.00	"	-1.706
7.116	1.50	2.00	4.001	8.76	6.14	1.97	"	-1.175
7.169	1.44	1.68	3.990	1.04×10^{-9}	5.48	1.95	"	-0.689
7.275	1.38	1.33	3.975	1.37	5.01	1.92	0.739	-0.372
7.488	1.33	1.12	3.965	1.76	3.94	1.91	0.738	-0.027

TABLE 7 (continued)

Time (yrs.)	R/R_{\odot}	L/L_{\odot}	$\log T_e$	$\rho_{ph} \left(\frac{gm}{cm^3} \right)$	$\rho_c \left(\frac{gm}{cm^3} \right)$	T_c	X_1	L_g/L
7.804	1.30	1.16	3.973	1.55	5.48	1.96	"	+ .263
8.44	1.22	1.30	3.999	1.21	6.90	2.09	"	+ .319
9.70	1.17	1.22	4.001	1.26	7.06	2.14	.737	+ .047
1.22×10^7	1.16	1.17	3.998	1.31	7.06	2.14	.736	+ .006
1.70	1.16	1.14	3.996	1.35	7.11	2.13	.733	+ .004
2.39	1.16	1.10	3.992	1.41	7.16	2.13	.729	+ .004
3.57	1.17	1.05	3.986	1.51	7.26	2.12	.722	+ .004
5.78	1.17	9.74×10^0	3.976	1.70	7.44	2.10	.710	+ .003
1.02×10^8	1.19	8.58	3.959	2.38	7.74	2.08	.689	+ .003
1.91	1.22	7.15	3.933	4.47	8.24	2.04	.653	+ .002
3.54	1.28	5.82	3.901	9.17	9.03	2.01	.593	+ .001
7.18	1.40	4.46	3.852	2.23×10^{-8}	1.06×10^2	2.00	.473	+ .001
1.40×10^9	1.52	3.43	3.806	4.75	1.40	2.07	.263	0.000
1.69	1.53	3.11	3.794	5.82	1.61	2.12	.173	0.000
1.88	1.53	2.93	3.768	6.50	1.80	2.17	.114	0.001
2.18	1.54	2.80	3.751	7.18	2.27	2.31	.036	0.000
2.45	1.60	3.38	3.794	5.40	4.98	2.69	.001	- 0.044

TABLE 8

The physical characteristics at the boundaries of the radiative and convective regions for evolutionary models with varying G and beginning of evolution at a universe age $T_0 = 0.1 \times 10^9$ years.

Time (yrs.)	M_{core}/M		r_{core}/R		T_b (°K)		ρ_b (gm/cm ³)	
	conv.	rad.	conv.	rad.	conv.	rad.	conv.	rad.
8.31×10^5		.19		.33		3.11×10^6		3.72×10^{-1}
1.66×10^6		.46		.48		3.02		4.61
3.32		.77		.60		2.67		3.53
4.99		.95		.70		1.86		7.83×10^{-2}
5.82		.99		.80		1.00		7.43×10^{-3}
7.0625								
7.0633	.02		.04		1.83×10^7		8.40×10	
7.0642	.03		.05		1.77		7.75	
7.0658	.06		.07		1.70		6.95	
7.0691	.10		.08		1.61		6.00	
7.0758	.15		.10		1.51		4.97	
7.089	.20		.12		1.40		4.06	
7.116	.25		.13		1.33		3.37	
7.169	.28		.15		1.27		2.88	

TABLE 8 (continued)

Time (yrs.)	M _{core} /M		r _{core} /R		T _b (°K)		ρ _b (gm/cm ³)	
	conv.	rad.	conv.	rad.	conv.	rad.	conv.	rad.
7.275	.27		.16		1.28		2.71	
7.488	.21		.15		1.38		3.01	
7.804	.16		.13		1.50		3.66	
8.44	.12		.12		1.68		4.95	
9.70	.15		.13		1.64		4.76	
1.22 x 10 ⁷	.17		.14		1.62		4.64	
1.70	.17		.14		1.62		4.67	
2.39	.17		.14		1.61		4.70	
3.57	.17		.14		1.60		4.77	
5.78	.16		.13		1.59		4.90	
1.02 x 10 ⁸	.16		.13		1.58		5.12	
1.91	.15		.12		1.56		5.49	
3.54	.13		.11		1.55		6.07	
7.18	.11		.09		1.54		7.29	
1.40 x 10 ⁹	.09		.07		1.58		9.29	

TABLE 8 (continued)

Time (yrs.)	M _{core} /M		r _{core} /R		T _b (°K)		ρ _b (gm/cm ³)	
	conv.	rad.	conv.	rad.	conv.	rad.	conv.	rad.
1.69	.08		.06		1.59		1.05 × 10 ²	
1.88	.07		.06		1.61		1.14	
2.18	.07		.05		1.68		1.41	
2.45	.02		.03		2.24		3.78	

Figure Captions

- Figure 1: The variation of the gravitational coupling coefficient G with time. $G(\text{now}) = 6.67 \times 10^{-8} \text{ dynes cm}^2/\text{gm}^2$.
- Figure 2: Evolutionary track for the sun. The solid line is calculated with G varying in time. The dashed line represents the evolution of the sun with constant G . The crosses on the tracks correspond to the points at which the central hydrogen has been depleted in the sun.
- Figure 3: The ratios of the net rates of destruction of hydrogen by two branches of the proton-proton chain, for varying G and constant G , very early in the main-sequence solar evolution.
- Figure 4: Helium concentration by mass as a function of mass fraction, in the present sun, for both varying G and constant G cases.
- Figure 5: Helium concentration by mass as a function of mass fraction, for varying G and constant G models having central hydrogen just depleted.
- Figure 6: The luminosity-effective temperature diagram for a one solar mass star starting evolution at the indicated universe ages.

Figure 7: The fraction by mass of helium in the sun when central hydrogen is just depleted. Each curve represents the indicated universe ages for the beginning of stellar evolution.

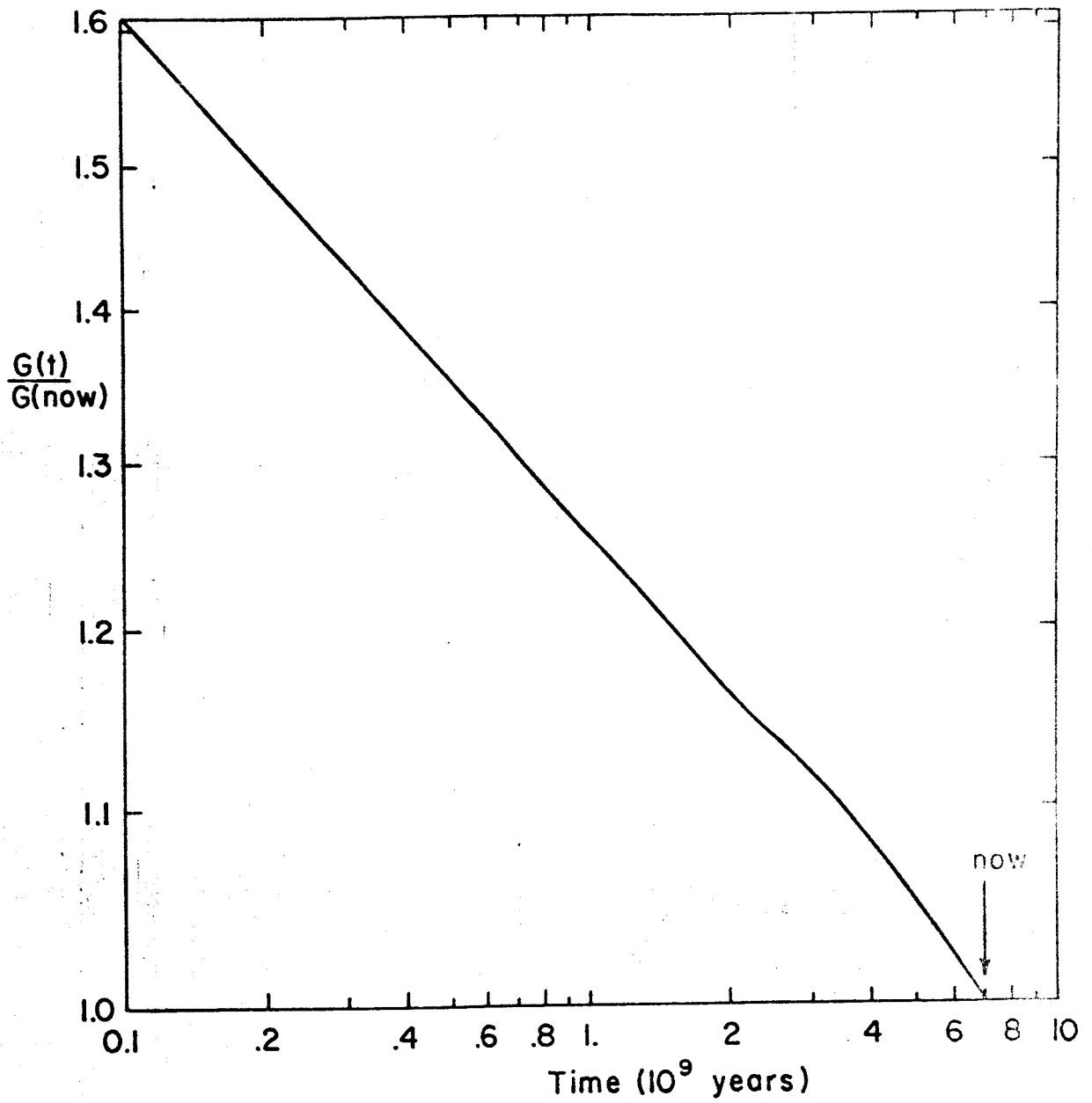


Figure 1

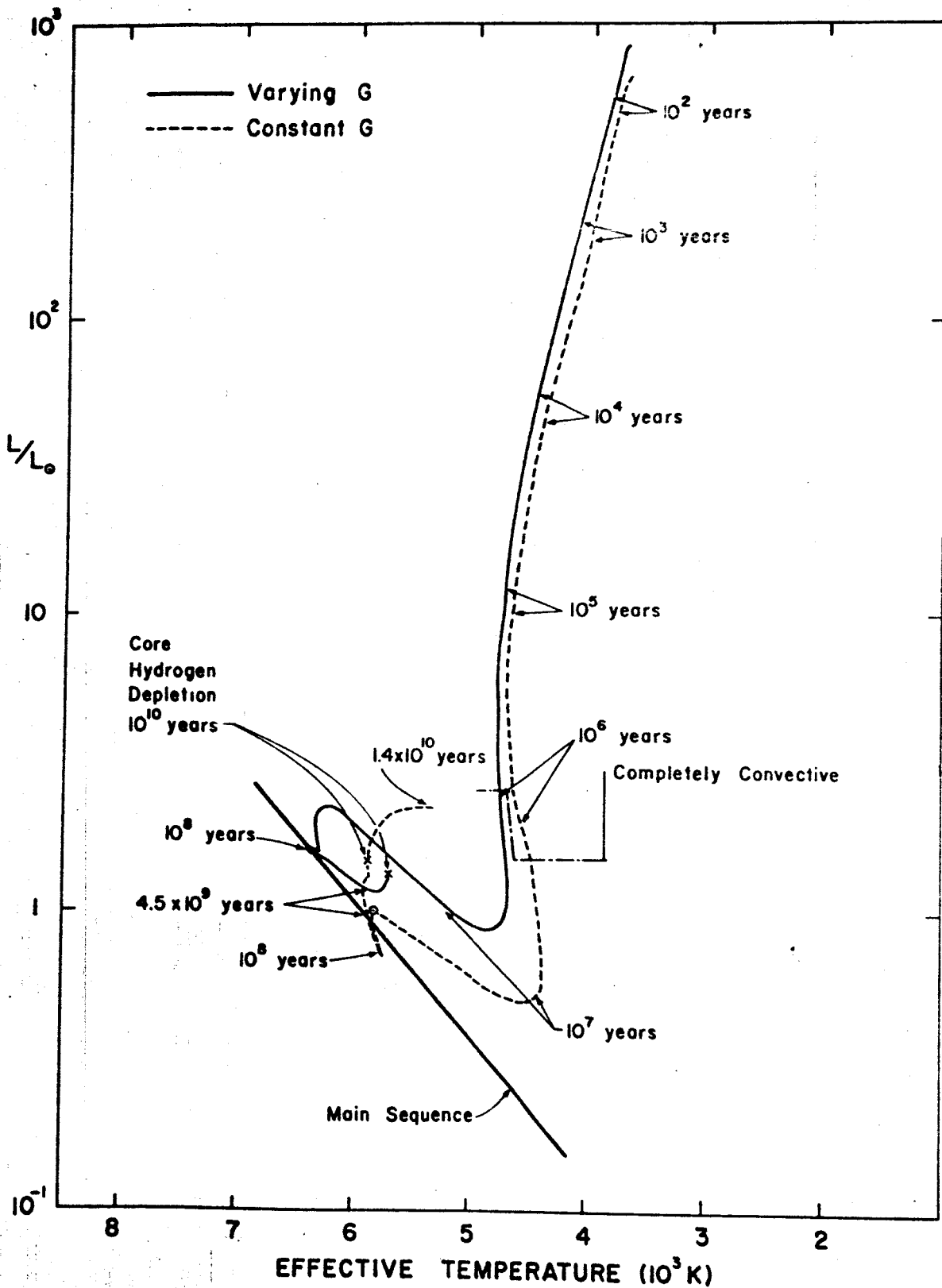


Figure 2

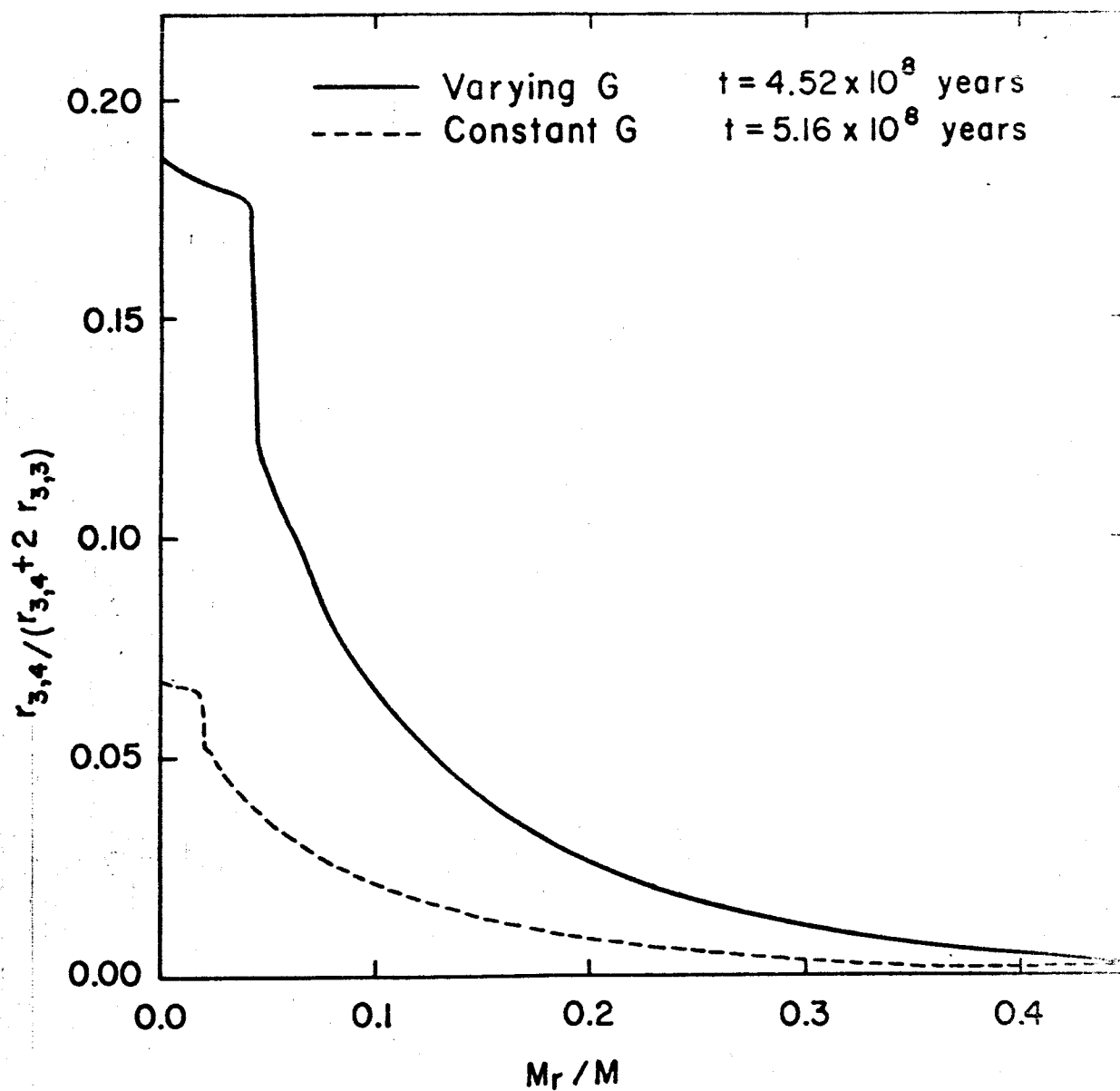


Figure 3

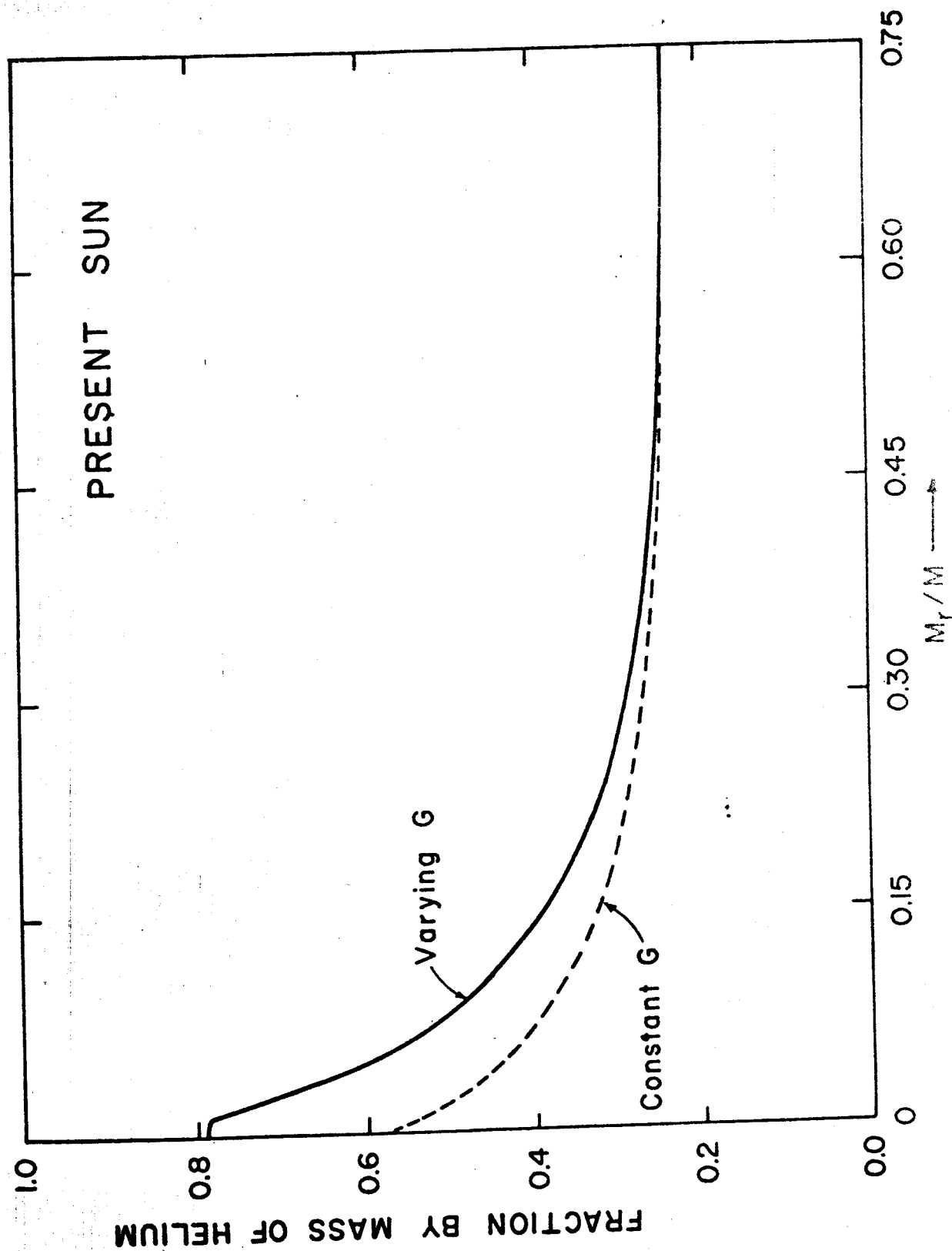
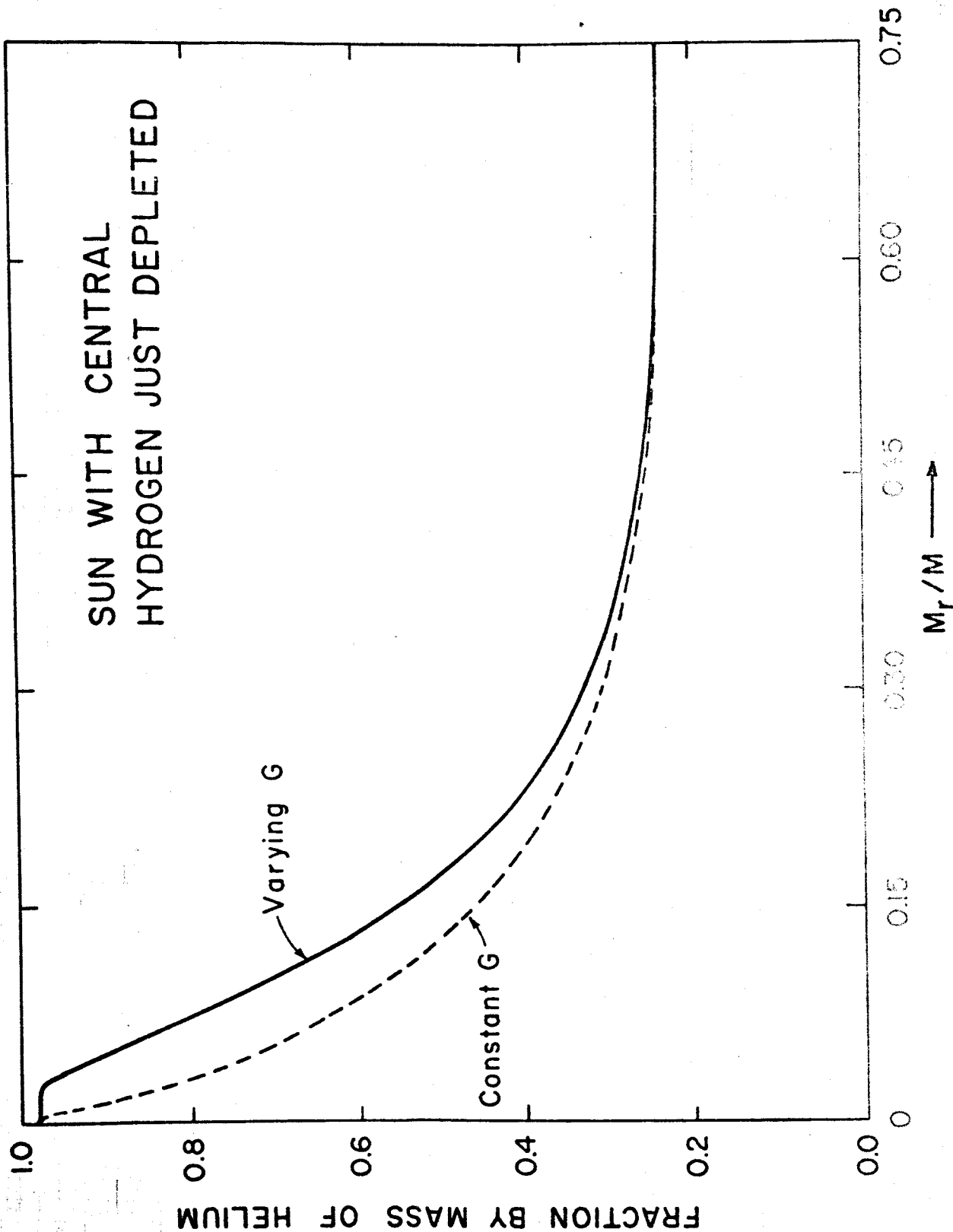


Figure 4

XERO COPY

XERO COPY

XERO COPY



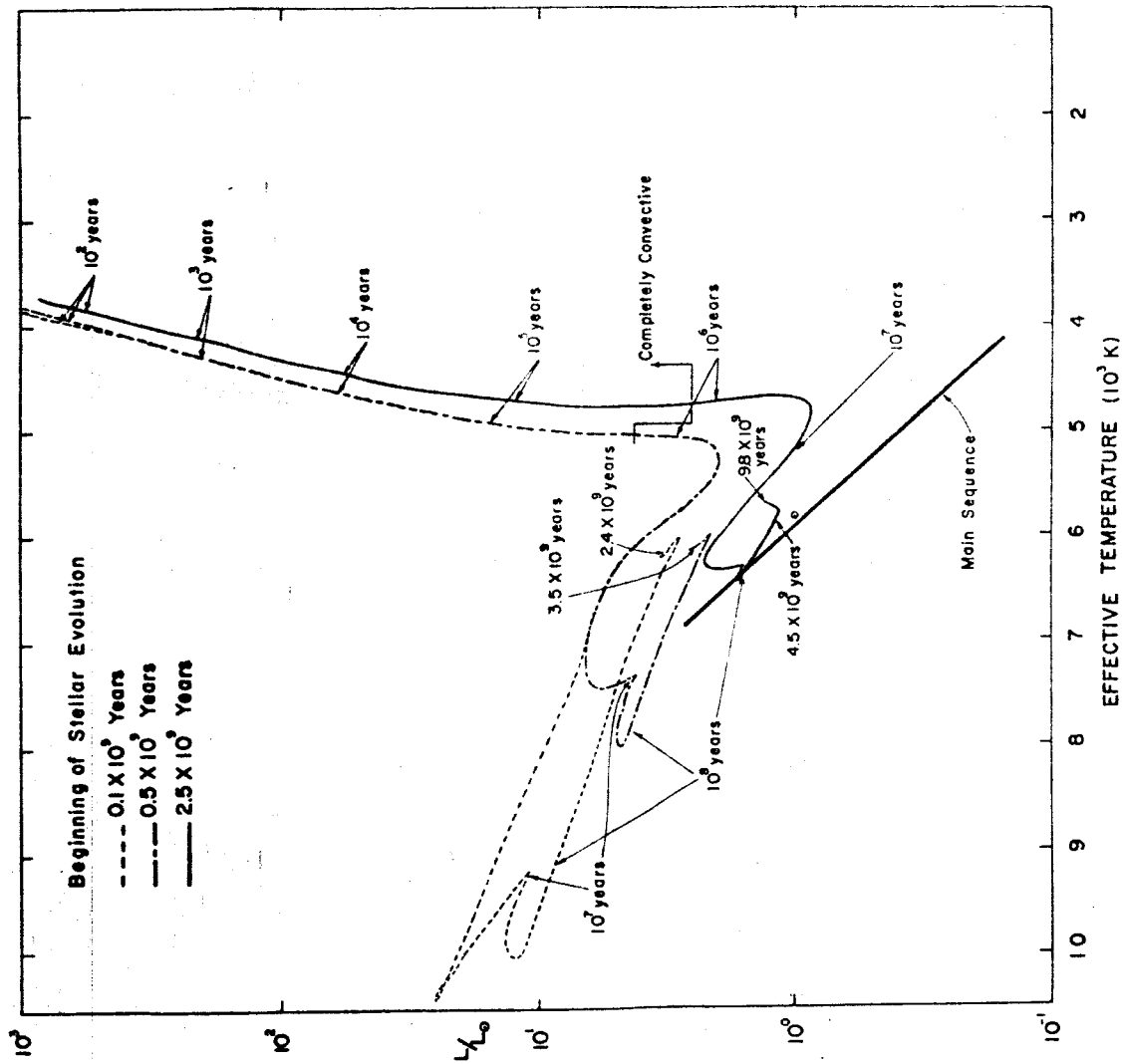


Figure 6

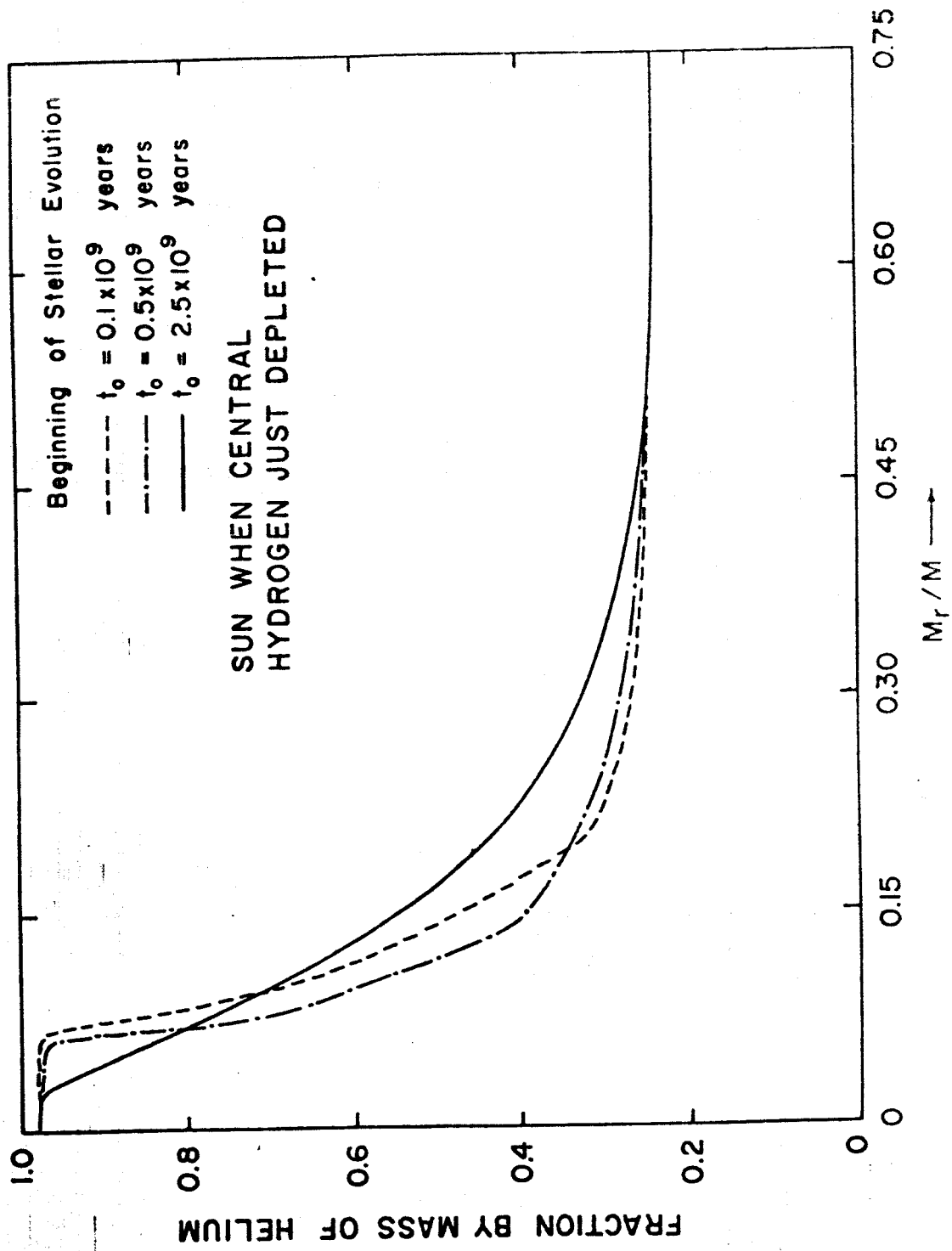


Figure 7